J.W. PARK*, B.H. KO*, W.Y. JUNG*, D.K. PARK**, I.S. AHN*#

THE HIGH TEMPERATURE OXIDATION STABILITY OF STS434L/SILICON OXIDE COMPACTS

In order to improve the high-temperature oxidation stability, a study of 434L sintered stainless steel was focused on the effect of addition of metallic oxides to form stable oxide film on the inner particle surface. In this paper, oxidation behavior of 434L compacted parts in accordance with the addition of metallic oxides were discussed with high temperature oxidative reaction, and sintering behavior analysis under 950°C. Oxidation weight gains of 434 L have increased as a form of parabolic laws. The high-temperature oxidation resistance was improved by the mixed addition of amorphous SiO_2 and silica up to 2wt.%. The oxidation rate was decreased and kept constant after 60 hours. It was caused by the restraint succeeding oxidation due to the stable oxide formation of Cr_2SiO_4 phases on the particle surface to prevent densification and inhibition the external diffusion of Cr. High-temperature stability was confirmed by the electrical resistivity maintains the constant value of 1.3×10^{-2} $\Omega \cdot cm$ when the silica added less than 2w/o to 1w/o A-SiO_2 added 434L.

Keyword: High-temperature oxidation stability, metallic oxide, densification

1. Introduction

Recently in accordance with demand for miniaturization and firsthand, necessity of indirect heating method of resistant materials has spread instead of direct heating system. When the heat transfer by radiation, it takes a long heating by indirect heating method of the heating element time and low efficiency at low-temperature region due to high electrical resistivity requirement. However, the direct heating method has an advantage that can be firsthand of electrical equipment and unified process of high electrical resistivity component is not restricted to the length and width of the heater. General traditional manufacturing method can not satisfy demand for integrated and minimized heating unit, so powder metallurgy method using the powder material has been raised for the most useful method for manufacturing. In case of applying to the manufacturing of a high temperature heating element by P/M, it has issues to be considered but so far has not been studied almost. In order to use the sintered stainless steel at high temperature, the protective oxide should be formed well on the surface and be able to protect surface also oxide layer should be stable [1-3]. This protective layer is mainly related to the formation of Cr_2O_3 and subjected to growth stress in accordance with growth of oxide layer. Also, it generates thermal stress due to difference coefficient of expansion between matrix and oxide layer by repeated use of the heating and cooling. These stresses occur crack of oxide layer and flaking from matrix alloy. If it leads to destruction, forming element of scale which contained in matrix alloy diffuses to surface and regenerates the

scale that can protect material [4,5]. By the repeat of reaction, the element of the alloy to form a protective scale is exhausted and material is finally end of life. Many experiments have been progressed to improve the adhesion between oxide layer and base alloy to maintain the formed protective scale for long time [6-10]. According to A. Bautista, F. Velasco, the addition of elements that have larger affinity for oxygen than elements for forming oxide layer can improve the adhesion of oxide layer to the base alloy or increase high-temperature oxidation resistance by using coating method [11]. The other way to improve high-temperature oxidation resistance of materials is adding Al and Si. The formed metal oxide on the surface by adding strong oxidative metal element such as Al and Si play a role of the oxide layer of base alloy which can protect inner alloy at high temperature [4,5,10]. The formed Al_2O_3 layer not only control internal penetration of oxygen and outer diffusion of Al in matrix alloy but also avoid generating other oxide. However it has a disadvantage in economic term because this way need to a large amount of addition or decrease oxidation resistance at the time of exhaustion of Al [12-15]. On the other hand, it was reported that the addition of Si form Cr_2O_3 layer and the thin SiO_2 layer together and prevent the diffusion of various kinds of elements, it leads to enhance the oxidation resistance [15-17].

In the paper, the STS434L powder in ferritic stainless steel that has low coefficient of expansion and excellent high temperature oxidation resistance [18,19] mixed with amorphous and crystalline silica to inhibit the densification and investigate the effect of high-temperature oxidation stability.

* SCHOOL OF NANO AND ADVANCED MATERIALS SCIENCE & ENGINEERING, GYEONGSANG NATIONAL UNIVERSITY, 900 GAJWA-DONG, JINJU, GYEONGNAM 660-701, KOREA
** LINC, GYEONGSANG NATIONAL UNIVERSITY, 900 GAJWA-DONG, JINJU, GYEONGNAM 660-701, KOREA
# Corresponding author: ais@gnu.ac.kr

2. Experimental procedure

In this study used STS; stainless steel (Korea Standard) 434L Powder, of Daido Corporation(Japan) and the used metallic oxide that the average particle size of SiO_2 oxide powder is 10 μm, and the purity is 99.9% made by Alfa Junsei Chemical Co. LTD(Japan). The used sodium silicate to gain amorphous silica is water soluble silicate and its mole ratio of SiO_2 / Na_2O is 1.032. The STS434L powder having composition shown in table 1 was mixed with sodium silicate up to 10w/o to obtain 2.5w/o amorphous silica. Also, the 1w/o amorphous silica fixed and crystalline SiO_2 up to 4w/o were added to 434L powder and mixed by SPEX Mill for 2 hrs. Curing of amorphous silica mixed STS434L powder was carried at 350°C for 3 hrs in order to remove water from the result of TGA analysis for sodium silicate. Mixed powder was compacted with 730 MPa to form rectangular bar type of 50×4×4 mm dimension. The green compacts blended amorphous silica(A-SiO_2) and crystalline SiO_2 with STS434L were preheated to 300°C with 30°C/min heating rate for 10 mins. These compacts were consecutively heated to 950°C with heating rate of 15°C/min, and then maintained for 210 hrs in air atmosphere. Air cooled specimens were weighed to investigate the oxidation behavior after respective holding time. The formed each oxide layer and distribution were analyzed by EDS mapping and the phase change of the generated oxides was also observed through the X-ray diffraction meter. The density was measured by Archimedes' principle. In addition, it was compared with electrical resistivity to investigate the high temperature stability. The electrical resistance was measured by using the electrical resistivity device 'Hioki 3540' model after surface polishing and silver paste covering at both sides of specimens to minimize the contact resistance.

TABLE 1

Composition of the used stainless steel powder (wt.%)

	C	Cr	Ni	Mo	Si	Mn	Cu	Fe
434L	0.01	16.73	—	1.09	0.8	0.17	—	Bal

3. Results and discussion

TABLE 2

Absolute values of weight gain of four samples (g)

	10h	20h	30h	60h	90h	120h	150h	180h	210h
434L	0.23	0.26	0.28	0.31	0.35	0.37	0.4	0.41	0.42
434L/1w/o A-SiO_2	0.26	0.3	0.31	0.34	0.39	0.4	0.41	0.43	0.45
434L/1.75w/o A-SiO_2	0.32	0.35	0.38	0.43	0.44	0.46	0.46	0.46	0.52
434L/2.5w/o A-SiO_2	0.4	0.47	0.51	0.52	0.56	0.57	0.62	0.63	0.65

Fig. 1 shows the TGA curve of sodium silicate which has the weight loss due to water evaporation upto 300°C, so

the curing of amorphous silica mixed STS434L powder was implemented at 350°C for 3 hrs in order to remove water. Fig. 2 shows (a) the weight change ratio and (b) relative density changes of STS434L green parts prepared by different addition of amorphous silica (A-SiO_2) in accordance with oxidation time up to 210 hrs at 950°C. Table 2 shows absolute values of weight gain of four samples. Oxidation weight gains of 434L have increased as a form of parabolic laws, which means that the oxide film grew according to the oxide diffusion through the densely formed oxide film. The weight change ratio (%) of all samples are greatly increased to 10 hrs and thereafter slowly increased upto 210 hrs. In case of the addition of A-SiO_2, the weight change slope were almost same values with that of 434L over 60 hrs, so adding A-SiO_2 has little effect on oxidation inhibition at high-temperature. It was reported that the added metallic oxide to form oxide layer has positively influence on high-temperature oxidation resistance by delaying the oxidation and protecting Cr-oxidation layer. However, Fig. 2a,b show continuous weight gain and density increase depending on the oxidation time in case of adding A-SiO_2. Therefore it is considered that the A-SiO_2 oxide during high-temperature oxidation test do not effectively restrain the densification by sintering. Also, the greater amount of A-SiO_2 in 434L occur high weight gain according to oxidation early on test. This is caused by the formability restraint and thereby providing more pores channel due to the relative density decrease as shown in Fig. 2b. X-ray diffraction pattern corresponding to respective specimens after different periods of oxidation time at 950°C in air is shown in Fig. 3. In XRD graph (a), even after oxidizing for 210 hrs, only peak α was observed and other oxide did not. The peak α decrease as the amount A-SiO_2 increase in 434L, while the other oxide such as Cr_2O_3, $(Fe_{0.6}Cr_{0.4})_2O_3$ appear as shown graph (c) and (d). From this result, it is determined that A-SiO_2 acts as the element to form various chromium oxide by promoting the oxidation of Fe and Cr. When adding 1.75 and 2.5% A-SiO_2 at high-temperature oxidation test for 210, peak SiO_2 was observed that it seemed to transform into crystalline. And the intensity of the oxide peak increases as the oxidation time get longer, also the oxide layer on particle surface could be consistently
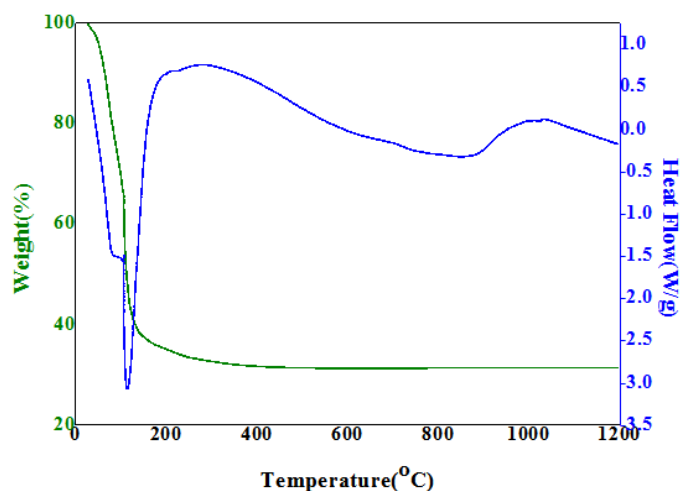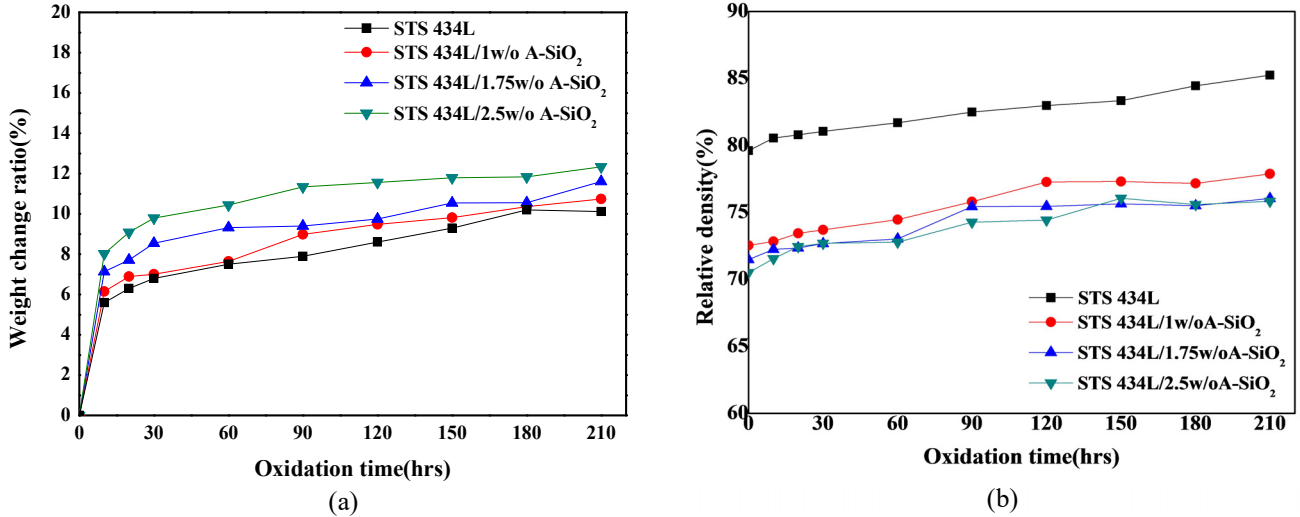

Fig. 1. TGA curve of sodium silicate

Fig. 2. Weight change ratio (a) and relative density (b) of amorphous SiO$_2$ added specimens after oxidation tests at 950°C for 210 hrs in air

formed by oxygen flow through pores channel. However, it is considered that the oxide layer did not sufficiently obstruct the densification at high-temperature. In other words, it was possible to slightly enhance the high-temperature oxidation resistance caused by adding A-SiO$_2$ to form oxide on surface but did not inhibit the oxidation weight gain and densification that occurs when maintained for a long time at high-temperature. Therefore,

it is necessary to form stable oxide layer without significantly reducing the moldability by minimal oxide addition to control particle size and maintain oxidation stability. The A-SiO$_2$ added 434L was shown to decrease the slope of the density variation after 120 hrs by changing A-SiO$_2$ to crystalline SiO$_2$ as shown in Fig. 3. It is expected to contribute to high-temperature oxidation stability by inhibiting particle densification. Therefore,
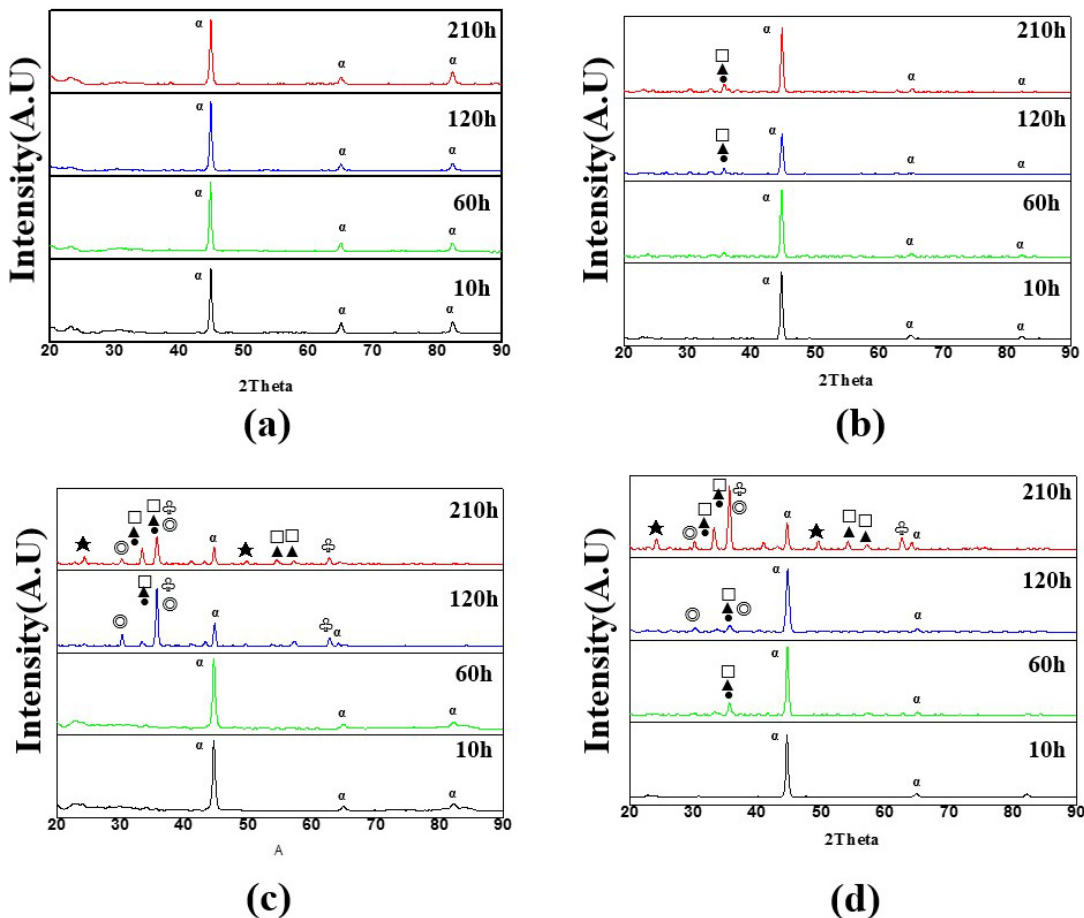

Fig. 3. X-ray diffractograms corresponding to respective specimens after different periods of exposure at 950°C in air : (a) STS 434L, (b) STS 434L/1w/o A-SiO$_2$, (c)STS 434L/1.75w/o A-SiO$_2$ and (d) STS 434L/2.5w/o A-SiO$_2$

oxidation stability of A-SiO$_2$ added 434L was investigated for further addition of crystalline silica. Fig. 4 shows the oxidation weight change ratio of 1w/o A-SiO$_2$ added 434L according to the crystalline silica addition. As shown in Fig. 4, the oxidation resistance of further addition of crystalline silica to 434L generally increases than that of only 1w/o A-SiO$_2$ added 434L. The addition of crystalline silica less than 2w/o had almost little weight gain after 90 hours and almost constant value has shown even after 120 hours. When the addition of crystalline silica, the relative density was slightly lower than that of 1w/o A-SiO$_2$
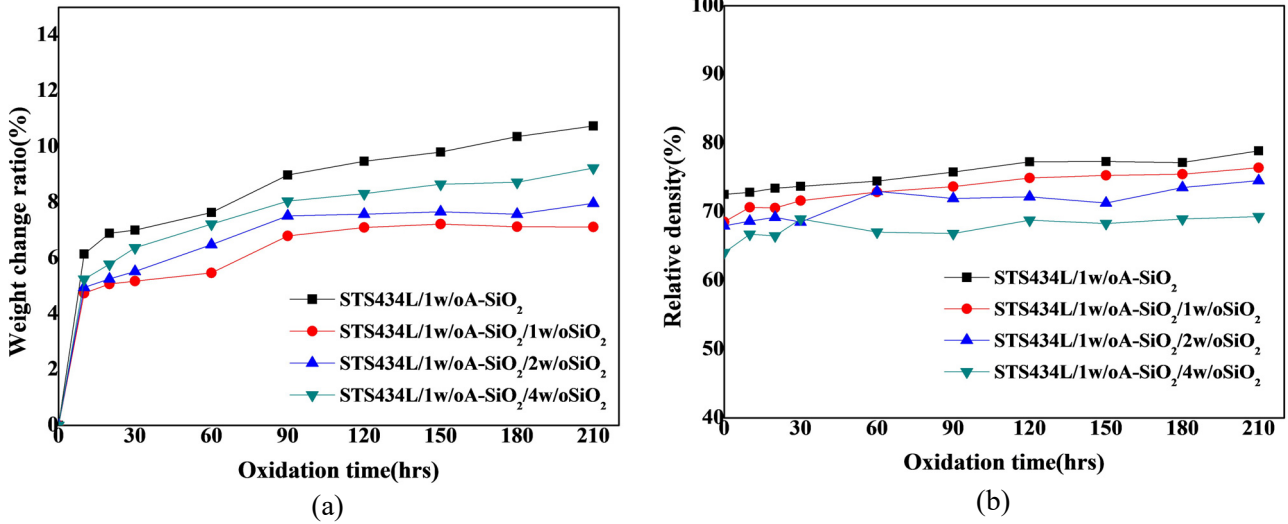

Fig. 4. Weight change ratio (a) and relative density (b) SiO$_2$ added to 1w/o A-SiO$_2$ fixed STS434L specimens after oxidation tests at 950°C for 210 hrs in air
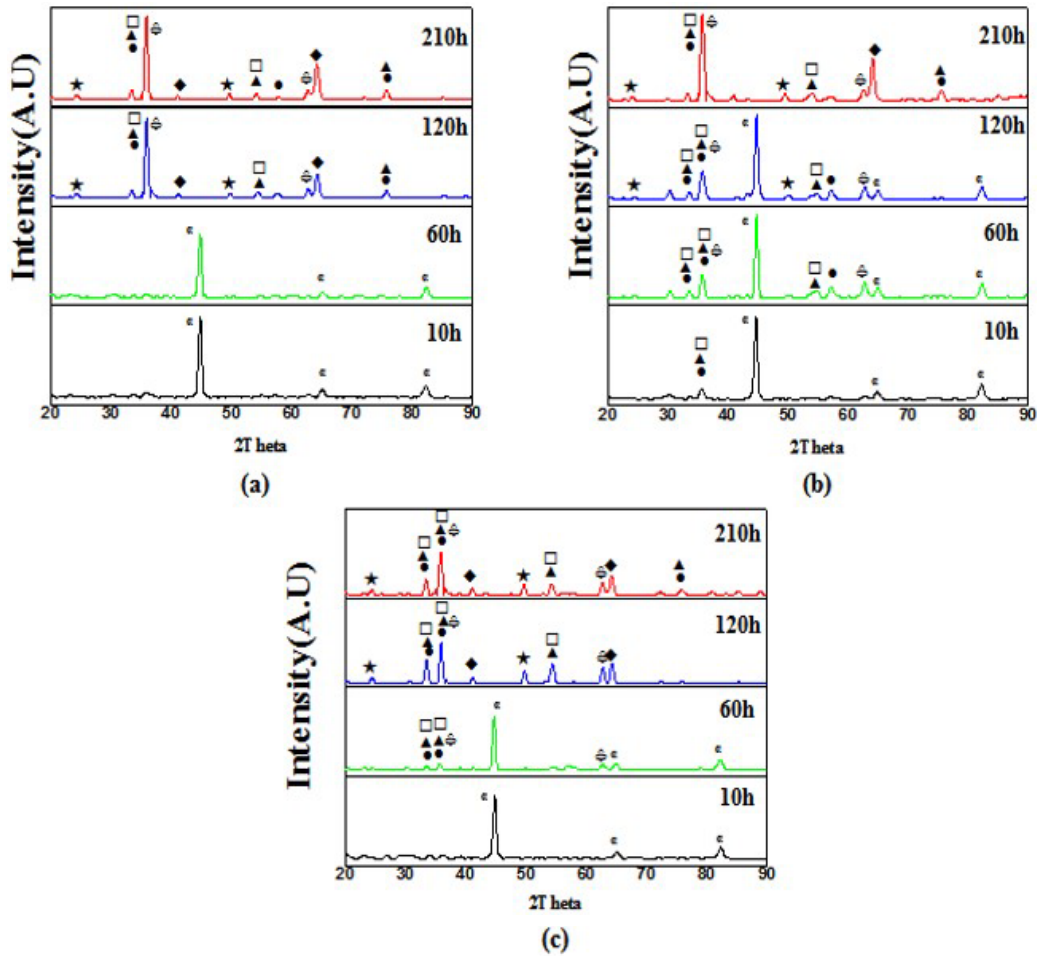

Fig. 5. X-ray diffractograms corresponding to respective specimens after different periods of exposure at 950°C in air: (a) STS 434L/1w/oA-SiO$_2$/1w/oSiO$_2$, (b) STS 434L/A-SiO$_2$/2w/oSiO$_2$, (c) STS 434L/A-SiO$_2$/4w/oSiO$_2$

added 434L but the almost little weight change behavior was observed from the initial stages of 30 hrs oxidation.

Fig. 5 shows XRD graphs of 1w/o A-SiO$_2$ added 434L estimated by varying the amount of silica after different time of oxidation test. The several kinds of oxide were formed as the oxidation time longer than 60 hours. In particular, the Cr-Si oxide was formed by adding crystalline silica, and relative reduction of α peak was observed while the amounts of Cr oxide increased. When the addition of the silica, the Cr oxide phases such as Cr$_2$SiO$_4$ are generated as oxidation time increases and form the stable oxide layer, and also it plays a role of protective scale formation not to make more defects or cracks on the powder surface. It is considered that no more densification between particles was caused by stable necking and stable oxide layer formation after 120 hours at high-temperature. The oxide layer stability was reviewed by measuring electrical resistance. Fig. 6 shows the electrical resistivity of the specimens for each oxidation time. Electrical resistivity has dramatically declined over 60 hrs of oxidation in case of the addition A-SiO$_2$ only. After the 90 hours, it was declined slowly and appeared 5×10^{-4} Ω·cm like the previous STS 434L [20]. This shows that the sintering was gradually proceeded with the flow of oxidation time. However the electrical resistivity was rapidly declined over 30 hrs, and those maintain the constant value of 1.3×10^{-2} Ω·cm after the 60 hrs when adding A-SiO$_2$ and crystalline silica at once.
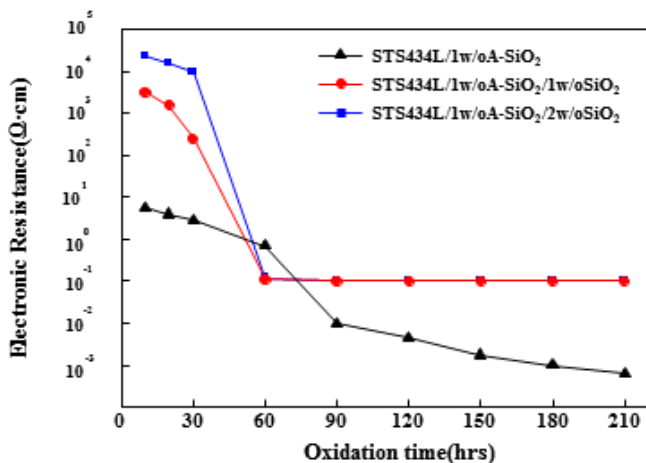

Fig. 6. Electrical resistivity of SiO$_2$ added to 1w/o A-SiO$_2$ fixed STS434L specimens after oxidation tests at 950°C for 210 hrs in air

Fig. 7 shows the relationship between weight change ratio after oxidation tests at 950°C for 210 hrs in air and relative green compact density of A-SiO$_2$ or SiO$_2$ added 434L. When compared to the high temperature oxidation resistance until 210 hrs in accordance with the relative density of the green compacts, the oxidation resistance of 434L/A-SiO$_2$/SiO$_2$ improved than that of 434L/A-SiO$_2$, even if the density of green compacts of 434L/A-SiO$_2$/SiO$_2$ were low. In other words, the A-SiO$_2$ and silica added 434L was more stable high temperature oxidation resistance at the same density. The crystalline silica inhibits the densification at the initial oxidation step and is considered that
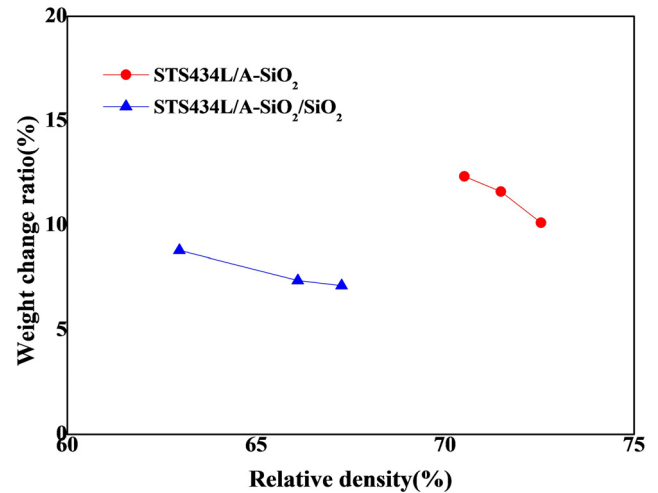

Fig. 7. The relationship between weight change ratio and relative compact density of A-SiO$_2$ or SiO$_2$ added specimens after oxidation tests at 950°C for 210 hrs in air

the oxide scales such as Cr$_2$SiO$_4$ which play a role of stable protective layer maintains high-temperature oxidation stability after 120 hrs.

Fig. 8 shows EDS mapping result of 434L with 1w/oA-SiO$_2$ and further added crystalline silica after 210 hrs exposure at 950°C. It was observed that the distribution of Si and O are concentrated in the grain boundary as shown in Fig. 8. In case of A-SiO$_2$ only added, the most of Cr in matrix was diffused to grain boundary, however, the Cr was evenly distributed in matrix and grain boundary by adding crystalline silica. Therefore, the oxidation stability is caused by the stable oxides formation such as Cr$_2$SiO$_4$ in grain boundary. And it inhibited the external diffusion of Cr and the critical concentration of Cr forming Cr oxides was reduced. As a result, the high-temperature oxidation stability could be maintained due to the formation of protective Cr$_2$SiO$_4$ oxide layer and Cr remaining in matrix.

4. Summary

The oxidation weight increasing rate was not changed in case of the addition of A-SiO$_2$ as compared with the 434L, and so adding A-SiO$_2$ has little effect on the oxidation inhibition at high-temperature.

It could be considered that the addition of A-SiO$_2$ combined with silica effects better oxidation resistance by the formation of the stable protective oxide scale such as Cr$_2$SiO$_4$. High-temperature stability was confirmed by the electrical resistivity maintains the constant value of 1.3×10^{-2} Ω·cm when the silica added less than 2w/o to 1w/o A-SiO$_2$ added 434L.
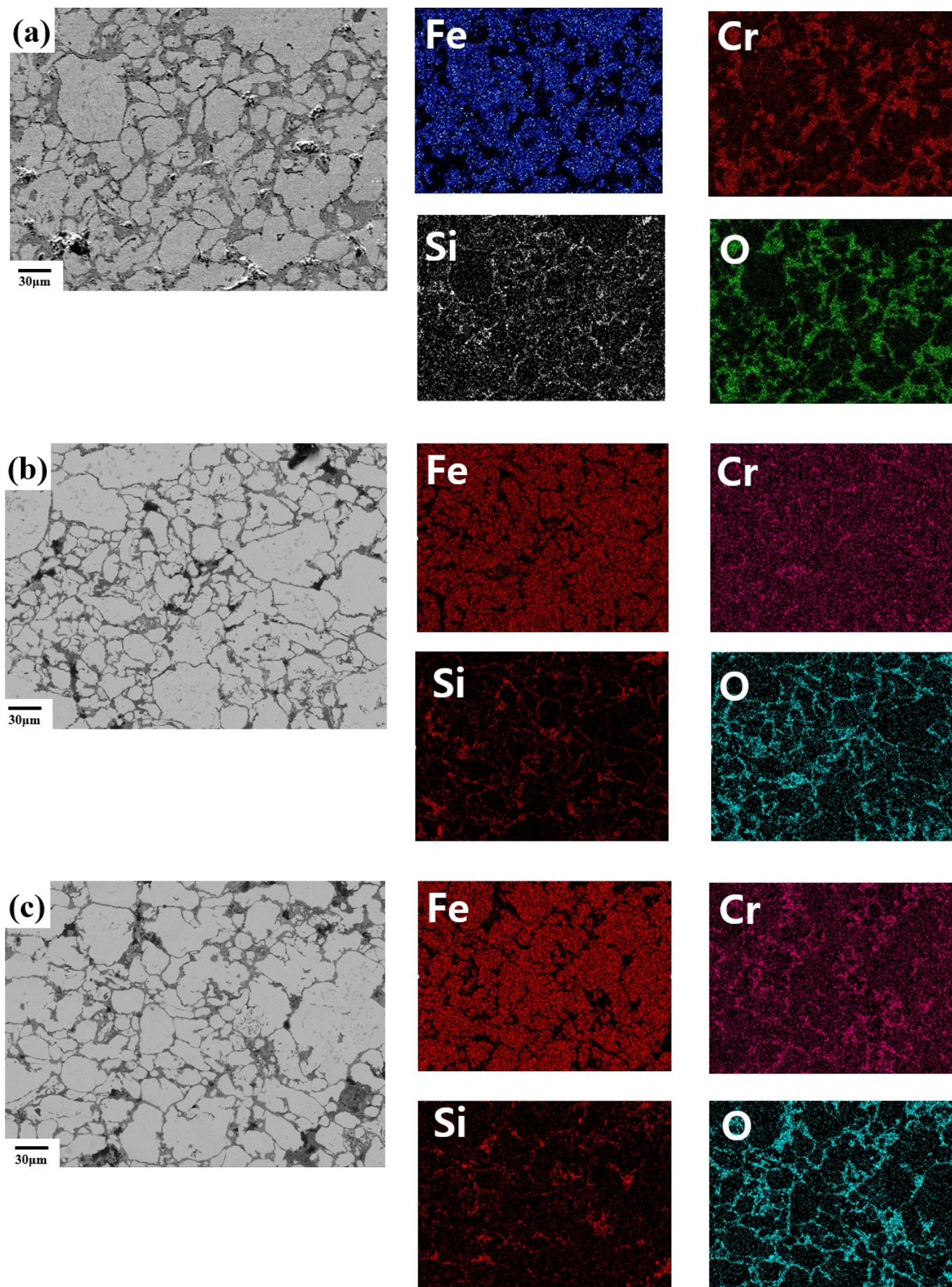
312

Fig. 8. The EDS mapping results of specimens after 210hr exposure at 950°C in air:STS434L/1w/oA-SiO$_2$, (b) STS434L/1w/oA-SiO$_2$/1w/oSiO$_2$ and (c) STS434L/1w/oA-SiO$_2$/2w/oSiO$_2$

REFERENCES

[1] J.H. Ryu, K.S. Lee, J. Corros. Sci. Soc. Tech. **21**, 69 (1992).

[2] H.S. Kim, J. Korean Powder Metall. Inst. **20**, 432 (2013).

[3] A. Tiziani, A. Molinari, L. Fedrizzi, A. Tomasi, P.L. Bronora, Corros. Sci. **45**, 672 (1990).

[4] A. Sharon, D. Itzhak, Mater. Sci. Eng. A. **224**, 177 (1997).

[5] S.. Chen, S. L. Kuan, W.T. Tsai, Corros. Sci. **48**, 634 (2006).

[6] F.H. Stott, G.C. Wood, J. Stringer, Oxid. Met. **44**, 113 (1995).

[7] B. Weiss, R. Stickler, Metall. Mater. Trans. A **3**, 851 (1972).

[8] A.V.C. Sobral, M.P. Hierro, F.J. Prez, W. Ristow Jr., C.V. Franco, Mater. Corros. **51**, 791 (2000).

[9] I.S. Lee, Korean. J. Met. Mater. **47**, 716 (2009).

[10] A. Rahmel, M. Schuetze, Oxid. Met. **38**, 255 (1992).

[11] A. Bautista, F. Velasco, J. Abenojar, Corros.Sci. **45**, 1343 (2002).

[12] T. Takalo, N. Suutala, T. Moisio, Metal. Trans. A. **10**, 1173 (1997).

[13] S.L. Park, Water glass coating on Ti surface for improved Cell Behaviors of Dental Implant (2012).

[14] O. Vedat Akgun, Mater. Sci. Eng. A. **203**, 324 (1995).

[15] G.C. Wood, Corros. Sci. **2**, 173 (1962).

[16] D. Caplan, M. Cohen, Corros. Sci. **15**, 141 (1959).

[17] T. Tanabe, S. Imoto, J. Japan Inst. Met. Mater. **9**, 507 (1979).

[18] J.P. Lee, J. Korean Powder. Metall. Inst. **22**, 271 (2015). (Korean).

[19] J.P. Lee, J. Korean Powder. Metall. Inst. **22**, 52 (2015). (Korean).

[20] J.W. Park, B.H. Ko, W.Y. Jung, D.K. Park, I.S. Ahn, Korean Powder. Metall. Inst. **23**, 1 (2016). (Korean).